

The effect of drying on wood fracture surfaces from specimens loaded in wet condition

G. Kifetew, F. Thuvander, L. Berglund, H. Lindberg

83

Summary The study describes the effect of drying on fracture surfaces of Scots pine *Pinus silvestris* L. Microtomed specimens of isolated and combined early- and latewood, in green and oven-dried/resoaked state were loaded to failure in uniaxial tension parallel to the grain. The fracture surfaces were studied using scanning electron microscopy (SEM). Both green early- and latewood samples showed rough fracture surfaces, which in latewood was dominated by intrawall failure. In the resoaked state, transwall failure dominated and fracture surfaces were more flat, indicating a more brittle fracture process. Although variation in the data was large, the strength of the resoaked samples were generally lower than those of paired green samples. The observations support irreversible cell wall damage formed during drying which severely affects the failure mechanism.

Introduction

Wood is a complex, heterogeneous and anisotropic material formed of cells varying in size, form and composition depending on the function they perform in the tree. Moreover the performance of wood derived from trees and utilized for construction purpose is entirely different after machining and drying. To date, discussions on damage have primarily been concerned with macrocracks induced during drying. The present study mainly concerns another phenomenon i.e. microscopic damage in the cell wall layers induced from drying.

The influence of structure on wood failure behaviour has been studied for a long time. Robinson (1920), Keith (1971), Dinwoodie (1974), Kucera and Bariska (1982) and Hoffmeyer (1990) utilized polarization microscopy, transmission electron microscopy (TEM) and/or scanning electron microscopy (SEM) to study

Received 8 July 1996

G. Kifetew
KTH-TRÅ, Wood Technology and Processing,
SE-100 44 Stockholm, Sweden

L. Berglund, F. Thuvander
Luleå University of Technology,
Division of Polymer Engineering, SE-97187 Luleå, Sweden

H. Lindberg
Luleå University of Technology
Dep. of Wood Technology
Skellefteå Campus
SE-93187 Skellefteå

Correspondence to: G. Kifetew

the cause and nature of failure and its relation to the anatomical structure of wood. Failure initiation as well as propagation under tension have been studied by many researchers and has been reviewed by Mark (1965, 1967).

Different terms have been introduced for descriptive purposes in characterizing features of the fracture surfaces in wood. Koran (1967, 1968) investigated the radial and tangential tracheid failure surface of black spruce loaded in tension perpendicular to grain at different temperatures. He used SEM to study the partially separated surfaces of wood and introduced the terms "intrawall" and "transwall" failure which will be used in the present study. By using SEM, DeBaise (1970, 1972) characterized the failure location within the cell wall and between wood cells by introducing terms like "intercellular" and "intracellular". According to Côté and Hanna (1983), three types of cell fracture are recognized; intercell, the separation of cells at the middle lamella; intrawall, within the secondary cell wall (usually at the S_1/S_2 interface or close to it); and transwall, fracture across the cell walls. These terms are illustrated in a schematic diagram in Fig. 1.

Let us first consider consequences of drying on the macroscale. During oven-drying from green condition, the tangential shrinkage of earlywood lies between 7% and 8%, while in the fiber direction it is *ca* 0.2% (Vintila 1939). The tangential shrinkage of the latewood is about 11% (Vintila 1939). The direction perpendicular to the microfibrils of the cell walls is a transverse direction and it is normal to the lumen surface. In this direction, the free shrinkage of the cell wall substance is about 20 to 30% (Boutelje 1962; Wallström et al. 1995).

At the microscale i.e. at the cell wall level, drying also has consequences. The wood cell or fiber is a natural composite made up of the middle lamella, primary wall and the three secondary cell wall layers with different orientations of microfibrils in relation to the fiber direction. The low gross longitudinal shrinkage depends mainly on the microfibril orientation of the S_2 layer which is almost parallel to the fiber direction. However, in the tangential direction, the S_2 layer, shrinks more than the S_1 and S_3 layers which are orientated in the ranges 50° to 70° and 60° to 90° with respect to the fiber direction respectively. The free shrinkage of the S_1 and S_3 layers in the longitudinal direction is expected to be high due to their microfibril orientation. However, due to the microfibril orientation in the S_2 layer, the shrinkage of the S_1 and S_3 are limited in the longitudinal direction. Thus due to drying, the different secondary cell wall layers would develop different stress distributions. In the tangential direction, the S_2 layer would force the S_1 and S_3 to shrink equally. This means that in the tangential direction, a tensile stress would arise in the S_2 and a compressive stress in the S_1 and S_3 layers (Fig. 2).

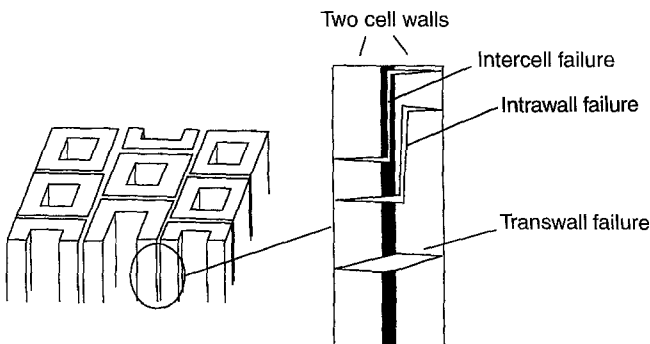


Fig. 1. Schematic diagram showing the different types of failure

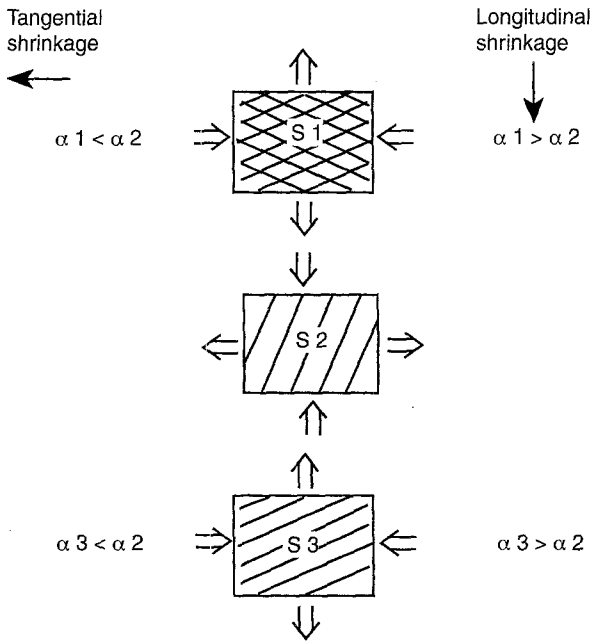


Fig. 2. Schematic representation of the stress distribution in the secondary cell wall due to drying: α_1 , α_2 and α_3 are the shrinkage in S₁, S₂ and S₃ respectively

Thuvander et al. (1996) calculated the drying stresses that would develop in the three secondary cell wall layers by treating the cell wall as a composite laminate with three plies (S₁, S₂ and S₃) with different thickness and microfibril orientation. As moisture diffuses from the material, the individual plies will change dimensions. However, these deformations are restricted by neighbouring plies with different microfibril orientations. Calculations revealed that the resulting drying stresses are likely to lead to cell wall damage in the S₁, S₂ and S₃ layers.

Salmén (1990) studied the effect of water as a plasticizing agent for lignin and carbohydrates and stated that the stress imposed on fibers or wood during drying will be relieved when the sample is immersed in water. Drying has in fact been used by Senfat and Bendsten (1985) to measure the microfibril angle of the S₂ layer. They even observed cell wall microchecks parallel to the microfibrils after repeated drying cycles. Despite the awareness of cell wall level drying stresses, the likelihood and significance of resulting cell wall damage has not been considered sufficiently.

In the literature, dried specimens are most often used in investigations of wood fracture phenomena. If cell wall damage is induced due to drying, the microstructure of such specimens is substantially different from green wood. All the reported observations of the mechanical behaviour of dry wood are then really based on materials with significant damage in the microstructure. The nature of the cell wall damage may be sensitive to details of the drying procedure. Existing reports on characteristic behaviour of specific wood species in the dry state may therefore be influenced by details in the damage state.

The hypothesis of damage in the cell wall due to wood drying could have been tested if direct observation of the cell wall was a simple experiment. However, such investigations by environmental scanning electron microscopy of microtomed specimens did not provide the information required. The primary limitation of such a study lies in the damage artefacts that may be introduced in the cell

walls during specimen preparation by means of microtoming. Another problem is that the cell wall damage is likely to be more diffuse than regular cracks and therefore requires experimental methods with high resolution.

The objective of the present investigation was to test the hypothesis of cell wall damage due to wood drying by examining the fracture surface at the ultra-structural level. In addition, effects of such damage on fracture mechanisms were of interest. We used fracture surface analysis (fractography) to accomplish the aim of the present investigation. The failure process in wood is likely to be affected by any damage that might be induced in the material due to drying.

86

The present study was conducted on wet specimens. Green wood is not expected to have any cell wall damage. In order to compare oven-dried specimens with green wood, observations need to be conducted at a comparable state. Therefore the oven-dried samples were immersed in water (resoaked) in order for them to reach a comparable state as the matched green specimens.

Material and methods

Five isolated early- and latewood and ten combined early- and latewood samples of normal grown Scots pine (*Pinus silvestris*) were cut in green condition using a sliding microtome along the fiber direction (Fig. 3). The thin rectangular specimens varied between 0.18–0.56 mm in thickness, *ca* 10 mm in width and 30 mm in length.

Each specimen of the isolated early- and latewood was split length-wise into two pieces and altogether five pairs of specimens were prepared. All the specimens were in green condition until they were divided into two groups. The first group of five specimens of each pair were preserved in the green condition. The second group of five specimens of the corresponding pair were oven-dried and then resoaked in water. Since a comparative study requires undamaged material, the behaviour of wood in the green state was investigated. To allow a realistic comparison, the oven-dried specimens were therefore resoaked in water and studied in the wet condition.

The tensile load was applied to all specimens when they were in the wet condition. Each end of the specimens were glued to aluminium sheets (Fig. 4) and the samples were loaded to failure through application of uniaxial tensile loading parallel to the fiber direction. The test was conducted with a load cell of 1 KN at a deformation rate of 20 mm/sec on a Reith Tensile Stage.

A total of 30 specimens including 10 isolated earlywood, 10 isolated latewood and 10 combined early- and latewood samples were loaded to failure. From a group of five samples only two randomly chosen specimens were used for fracture surface analysis. The corresponding paired specimens from the second group were then selected to match the specimens of the first group. Failed specimens were then air-dried and prepared for microscopic analysis. The fracture surface of failed specimens were examined at the ultrastructural level using a JEOL 5200

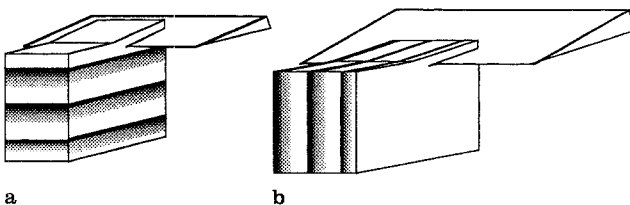


Fig. 3. Microtoming of specimens a) earlywood and latewood b) combined early- and latewood

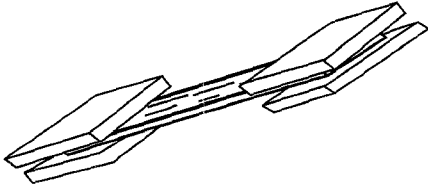


Fig. 4. Tensile test specimen

scanning electron microscope equipped with SEMAFORE image handling software.

Results and discussion

Fracture surface analysis

The three types of failure described by Côté and Hanna (1983) i.e. intercell, intrawall, and transwall failure were used to describe the different types of failure observed in this study see Fig. 1.

1. The earlywood fracture surfaces

The failure surfaces of the green isolated earlywood specimens demonstrated both transwall and intrawall failure. At a lower magnification, the fracture surface shows a rough appearance and is highly irregular (Fig. 5a).

In contrast, the resoaked specimens showed abrupt transwall fracture surfaces without any indication of intrawall failure (Fig. 6 a,b). The fracture surface, at low magnification is flat and showed much fewer features compared to the green specimens. Observations on the fracture surfaces of paired specimens of earlywood clearly demonstrated different failure characteristics for green and resoaked samples (Figs. 5a,b and 6a,b).

The importance of the microfibril angles of the S_1 and S_3 layers in the context of earlywood failure, has been emphasized by many researchers including Garland (1939). The earlywood layer is thinner and the microfibril angle of the S_2 layer is more inclined than in latewood cells. In earlywood, one-third of the cell wall belongs to layers other than S_2 (Cave 1968). The composition is also slightly different, earlywood has a higher percentage of lignin and hemicelluloses than latewood (Wellwood 1962).

Mark and Gillis (1970), pointed out that when wood layers are loaded in tension along the fiber direction, a high stress transverse to the microfibril direction would result in the S_1 layer. For this reason, they suggested that the S_1 layer is likely to be the source of failure initiation. In the resoaked samples, damage may cause earlier failure initiation. Also, the crack growth process is likely to be affected by cell wall damage. The green earlywood samples failed predominantly in transwall failure, probably initiated by the transverse stress in the S_1 layer. The S_2 layer, due to its microfibril orientation, is expected to hinder propagation of transwall failure as indicated by evidence for intrawall failure (Fig. 5a,b).

In the literature, it has been suggested that pits may be sites for failure initiation. In our fracture surface analysis we found no support for this suggestion. Our observations are in accordance with conclusions by Robinson (1920) and Mark (1967).

Studies of green earlywood fracture surfaces by Ifju and Kennedy (1962), Wellwood (1962) and Mark (1967) report a splintered, rough appearance, in

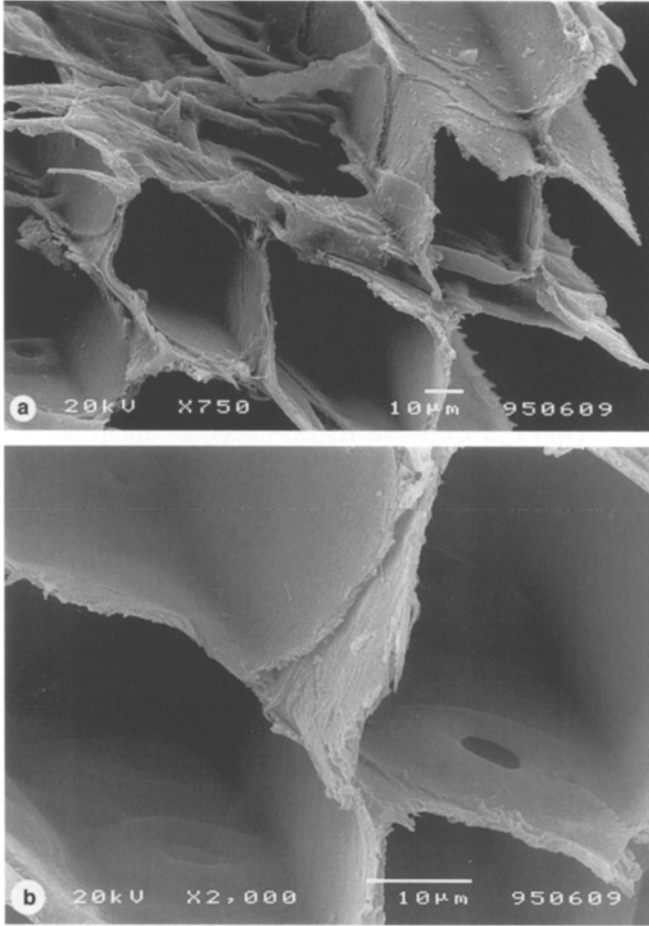


Fig. 5a,b. Micrographs of green earlywood

agreement with our results. In contrast to the green specimens, oven-dried earlywood in the dry state showed brush fracture surfaces in their studies. Although our oven-dried samples were resoaked and tested in the wet state, they also showed similar fracture surfaces as in the studies referred to.

2. The latewood fracture surfaces

In latewood specimens, the cell wall mainly consists of the S_2 layer and is much thicker than the earlywood. The microfibrils of the S_2 layer are almost fully aligned along the direction of the fiber. The fracture surface in the green latewood samples showed predominantly intrawall failure, most likely at the S_1/S_2 interface. The remaining part of the cell i.e. the S_2 and S_3 layers, have been drawn out several hundred microns in length (Fig. 7a). This produces a highly irregular and rough fracture surface.

For the resoaked specimens, transwall failure dominated. A slight unwinding phenomenon in S_2 was also observed (Fig. 8a) although this was also present in the green samples (Fig. 7a). Although the fracture surface is still rough for the resoaked specimens, very few cell layers were drawn out (Fig. 8b). This difference in behaviour is caused by changes in the structure introduced during drying of the samples.

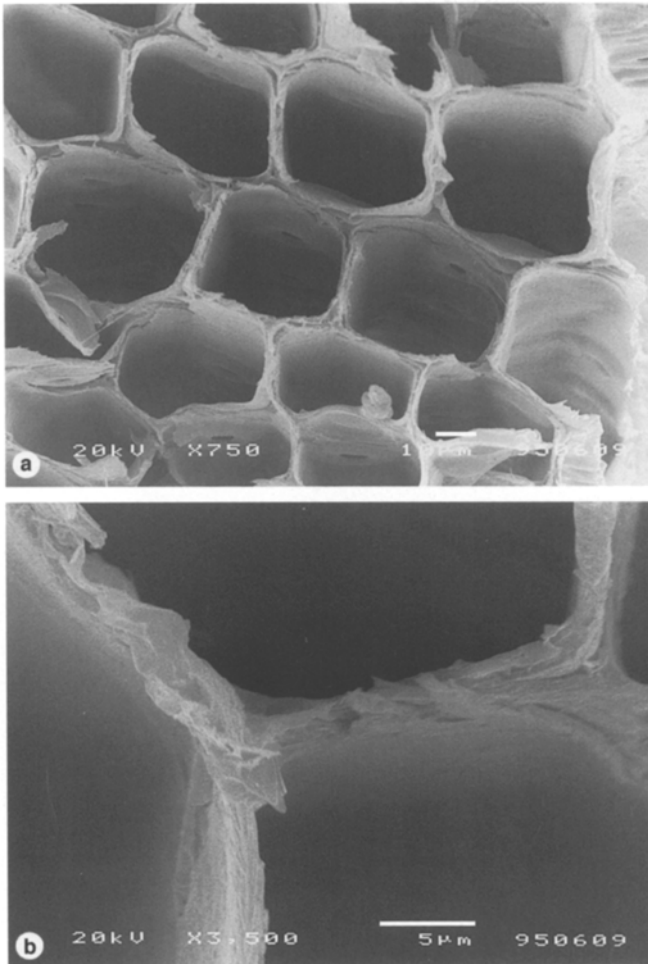


Fig. 6a,b. Micrographs of the resoaked earlywood

The failure behaviour of the cell wall in green latewood has been studied by other researchers. Garland (1939) observed the fracture surfaces of latewood and identified intrawall failure at the S_1/S_2 interface. Wardrop (1951) observed a splintering failure that usually followed the microfibril angle of the S_2 layers. The microfibril angle is also apparent from our micrographs (Fig. 7a). Ifju and Kennedy (1962) also observed failure that resulted in separation between the cells rather than across the cell walls. This would by the present terminology be termed intrawall failure. Our observations and interpretations of green latewood fracture surfaces is therefore in accordance with previous studies. However, no prior study of oven-dried/resoaked samples is known to us. It is therefore interesting to note that drying induces a more brittle fracture surface appearance in wet samples. The resoaked samples showed predominantly transwall failure with very little intrawall failure and very few cells which were drawn out to any significant length.

3. The combined early- and latewood fracture surfaces

Wood specimens i.e. with both the early- and latewood were also investigated (termed combined specimens). For the dried/resoaked specimens, the fracture

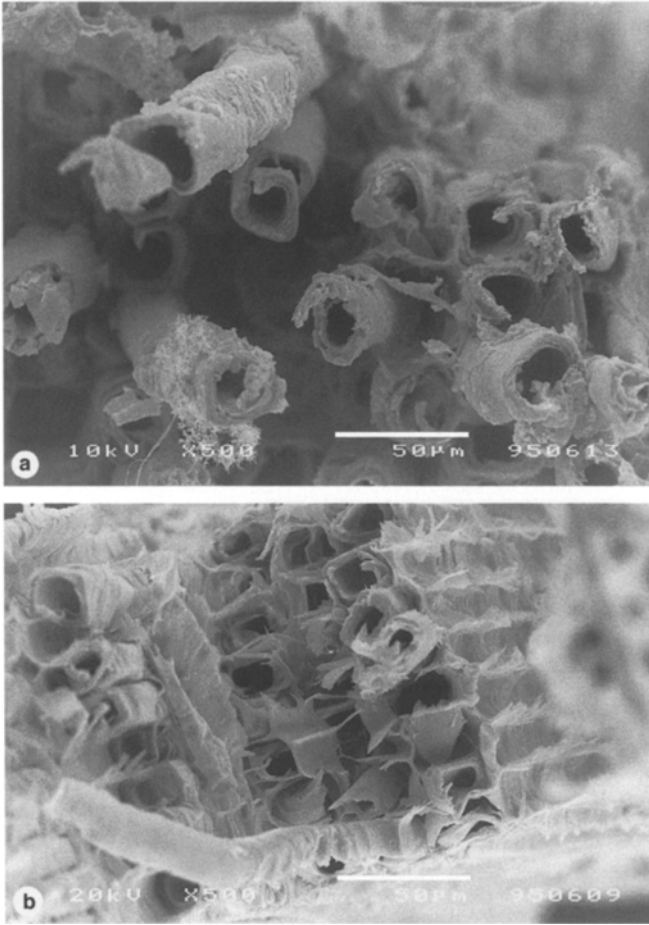


Fig. 7a,b. Micrographs of the green latewood

surface appearance was no different from the specimens of isolated earlywood or latewood layers. However, for the green specimens there was a significant difference. The earlywood in the combined specimens showed abrupt transwall failure and a much more featureless appearance than the isolated earlywood see Fig. 9. However, the fracture surfaces of the latewood region in combined green specimens exhibited fracture surfaces similar to those for green latewood in isolated specimens. It is therefore likely that failure was controlled by the latewood layer.

Since we do not have any quantitative values of failure strain, a discussion on fracture mechanisms in combined specimens will benefit from an estimate of the stress distribution between the early- and latewood regions. In this estimate, early- and latewood are considered as two separate but homogeneous phases. The volume fraction of the latewood v_L is assumed as 0.3. The modulus of elasticity of earlywood (E_E) is about 7 Gpa for latewood (E_L) 29 Gpa (Koponen et al. 1991).

The modulus of elasticity of combined early- and latewood (E_W) is according to the rule of mixtures:

$$E_W = v_L E_L + v_E E_E$$

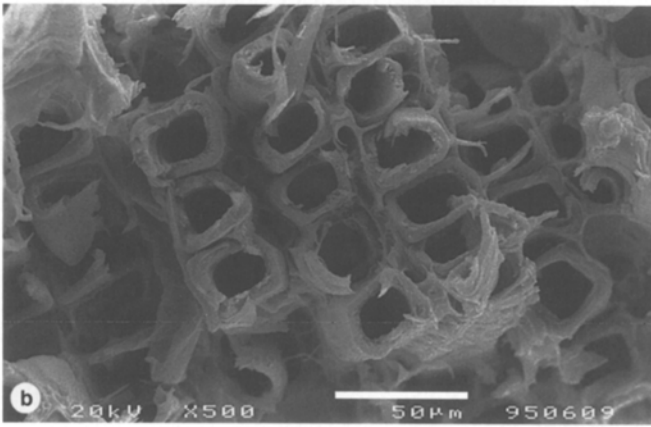
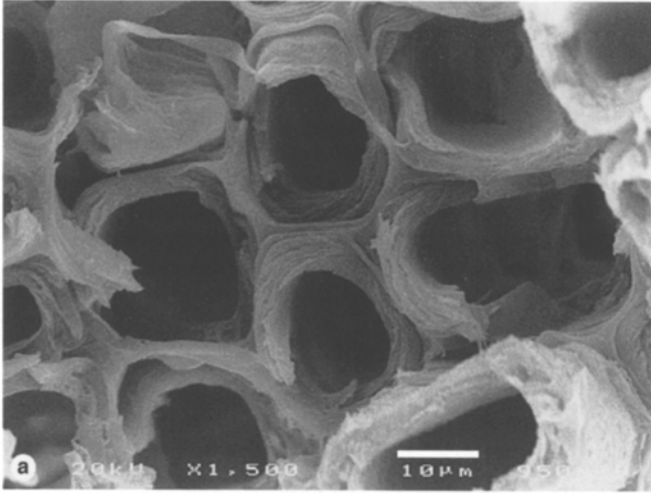


Fig. 8a,b. Micrographs of resoaked latewood

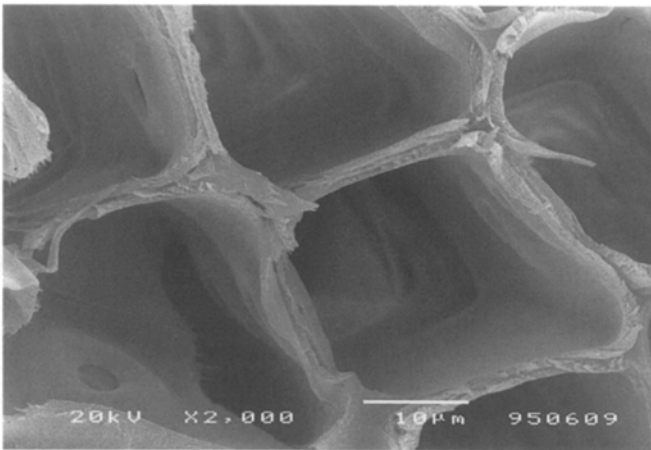


Fig. 9. Micrograph of the earlywood fracture surface in a combined early- latewood sample tested in green condition

Since strain is assumed to be equal in both the early- and latewood, the modulus of elasticity of wood E_W can be calculated as:

$$E_W = 0.3 * 29 + 0.7 * 7 = 13.6 \text{Gpa},$$

which is in agreement with typical experimental data.

At a given strain ϵ , the global wood stress (σ_W) would be:

$$\sigma_W = E_W \epsilon = \nu_L E_L \epsilon + \nu_E E_E \epsilon$$

92

The latewood layer would then carry the following portion of global wood stress:

$$\nu_L E_L \epsilon / E_W \epsilon = \frac{0.3 * 29}{13.6} = 64\% \text{ of the total stress.}$$

Sixty four percent of the total stress is carried by the latewood which constitutes only 30% of the cross-sectional area. The strain energy density is therefore much higher in latewood than in earlywood. Since the fracture surface in combined green latewood was similar to that observation in isolated specimens, fracture probably started in the latewood. As the major crack progressed into the green earlywood, excessive energy was released, a more brittle type of failure occurred and a flat fracture surface with transwall failure resulted. Such a mechanism explains why combined earlywood fracture surfaces look different than isolated green earlywood. The mechanism is supported by our estimate that latewood has a much higher strain energy density than the earlywood.

It is of interest to compare our observations with fracture surface results in the literature. Several other studies of wood fracture surfaces at moisture levels of about 10% are available for the same loading as used in the present study. Côté and Hanna (1983) characterized the fracture surface of southern pine. The earlywood layer showed an abrupt transwall failure, while latewood failure was intrawall which followed the S_2 microfibril angle. Sometimes the latewood layer failed in abrupt transwall failure and in other cases by intrawall failure by separation at the S_1/S_2 interface. Zink et al. (1994) analysed the fracture surface of southern pine and Douglas-fir. They found that the earlywood failure was abrupt transwall whereas latewood failed in combined transwall and intrawall failure. It is interesting to note that our dried/resoaked specimens showed similar fracture surfaces as those reported in the literature for wood at about 10% moisture content. Based on results in the present study, this indicates that the specimens used in previous studies showed a fracture behaviour characteristic of the damage state in the cell wall rather than that of the undamaged wood species in question.

Table 1 summarizes our fracture surface observations at the ultrastructural level. Transwall failure is favoured in dried/resoaked specimens. In addition, latewood cell wall layers in green specimens were drawn out several hundred microns in length whereas this phenomenon did not occur in dried/resoaked specimens. Drying has a dramatic effect on the fracture surfaces and therefore on the fracture mechanisms of wood. This is in support of the hypothesis that irreversible cell wall damage occurs during wood drying.

Finally, strength data for the tested samples are presented in Table 2. Reported samples are for pairs cut adjacent to each other. The major observation from the data is that, in general, the strength is lower for samples tested in the dried/resoaked state. The variation in the data is however significant. This is believed to arise from the use of very small samples which are cut with a microtome. Small samples are more likely to show density variations and also the microtoming

Table 1. Different types of failure

Wood layers		Green	Resoaked
Isolated	Earlywood	¹ Transwall + Intrawall	Transwall
	Latewood	¹ Intrawall + Transwall	¹ Transwall + Intrawall
Combined	Earlywood	¹ Transwall	Transwall
	Latewood	¹ Intrawall + Transwall	¹ Transwall + Intrawall

¹Dominating failure

Table 2. Tensile strength, (σ) for tested samples

Sample	Earlywood		Latewood		Combined early-latewood	
	Green σ [Mpa]	Resoaked σ [Mpa]	Green σ [Mpa]	Resoaked σ [Mpa]	Green σ [Mpa]	Resoaked σ [Mpa]
1	62	–	153	39	48	18
2	49	30	74	104	70	20
3	43	38	46	38	35	40
4	53	39	91	22	57	20
5	51	22	–	–	50	34

operation itself is likely to induce damage to the specimens. However, despite this limitation all sample pairs except two show the expected decrease in strength for the dried/resoaked specimen.

Conclusion

The present fracture surface study provides support for the hypothesis of irreversible cell wall damage from drying and demonstrates a strong effect on the failure mechanisms in the wet state. Both green earlywood and latewood showed rough fracture surfaces, which for latewood was dominated by intrawall failure. However, in the dried/resoaked state transwall failure dominated and fracture surfaces were more flat, indicating a more brittle fracture process. It is of significance that results in the literature on characteristic behaviour of specific wood species may be influenced by details in the damage state of the material.

References

- Boutelje J** (1962) On shrinkage and change in microscopic void volume during drying, as calculated from measurements on microtome cross section of Swedish pine (*Pinus silvestris* L.) Svensk Papperstidning 65(6): 209–215
- Cave ID** (1968) The anisotropic elasticity of the plant cell wall. Wood Sci. Technol. 2: 268–278
- Côté WA, Hanna RB** (1983) Ultrastructural characteristics of wood fracture surface. Wood and Fiber Science 15(2): 135–163
- DeBaise GR** (1970) Mechanics and morphology of wood shear fracture. Ph.D. Dissertation, State University of New York, Syracuse
- DeBaise GR** (1972) Morphology of wood shear fracture. J. Materials 7(4): 568–572
- Dinwoodie JM** (1974) Failure in timber, Part 2: The angle of shear through the cell wall during longitudinal compression stressing. Wood Sci. Technol. 8: 56–67

- Garland H** (1939) A microscopic study of coniferous wood in relation to its strength properties. *Annals of the Missouri Botanical Garden*. Vol. 26: 1–83
- Hoffmeyer P** (1990) Failure in wood as influenced by moisture and duration of load. Ph. D. Dissertation, State University of New York, Syracuse.
- Ifju G, Kennedy RW** (1962) Some variables affecting microtensile strength of Douglas-Fir. *Forest Products Journal* 12(5): 213–217
- Keith CT** (1971) The anatomy of compression failure in relation to creep-inducing stresses. *Wood Science* Vol. 4(2): 71–82
- Koponen S, Toratti T, Kanerva P** (1991) Modelling elastic and shrinkage properties of wood based on cell structure. *Wood Sci. Technol.* 25: 25–32
- Koran Z** (1967) Electron microscopy of radial tracheid surfaces of black spruce produced by tensile failure at various temperatures. *Tappi* Vol. 50, No 2: 60–67
- Koran Z** (1968) Electron microscopy of tangential tracheid surfaces of black spruce produced by tensile failure at various temperatures. *Svensk Papperstidning* Nr. 17: 568–576
- Kucera LJ, Bariska M** (1982) On the fracture morphology in wood. Part 1: A SEM-study of deformation in wood of spruce and aspen upon ultimate axial compression load. *Wood Sci. Technol.* 16: 241–259
- Mark R** (1965) Tensile stress analysis of cell walls of coniferous tracheids. Cellular ultra-structure of wood plants. Syracuse Univ. Press
- Mark R** (1967) Cell walls mechanics of tracheids. New Haven and London, Yale Univ. Press.
- Mark R, Gillis PP** (1970) New models in cell-wall mechanics. *Wood and Fiber* 2(2): 79–95
- Robinson W** (1920) The microscopical features of mechanical strains in timber and the bearing of these on the structure of the cell-wall plants. *Philos. Trans. Soc. London*. B210: 49–82
- Salmén L** (1990) On the interaction between moisture and wood fiber materials. Material interaction relevant to the pulp, paper and wood industries. (Caulfield DF; Passaretti JD, Sobczynski SF eds) *MRS Symp. Proc. Pittsburg*, vol 197, pp 193–205
- Senft JF, Bendsten BA** (1985) Measuring microfibrillar angles using light microscopy. *Wood and Fiber Science* 17(4): 564–567
- Thuvander F, Kifetew G, Berglund L** (1996) Modelling of cell wall drying stresses in wood.
- Vintila E** (1939) Untersuchungen über Raumgewicht und Schwindmaß von Früh- und Spätholz bei Nadelhölzern. *Holz Roh-Werkst* 2: 345–357
- Wallström L, Lindberg H, Johansson J** (1995) Wood surface stabilization. *Holz als Roh und Werkstoff* 53: 87–92
- Wardrop AB** (1951) Cell wall organization and the properties of the xylem I. Cell wall organization and the variation of breaking load in tension of the xylem in conifer stem. *Aust. J. Sci. Res.*, B4(4): 391–417
- Wellwood RW** (1962) Tensile testing of small wood samples. *Pulp and Paper Magazine of Canada*. 63(2): T62–T67
- Zink AG, Pellicane PJ, Shuler CE** (1994) Ultrastructural analysis of soft wood fracture surface. *Wood Sci. Technol.* 28: 329–338